Journal of Power Sources 218 (2012) 181–186

Contents lists available at SciVerse ScienceDirect

Journal of Power Sources

journal homepage: www.elsevier.com/locate/jpowsour

Influence of trace oxygen in low-crossover proton exchange membrane fuel cells

R. Paul Brooker [a,*], Marianne P. Rodgers [a], Leonard J. Bonville [a], H. Russell Kunz [b], Darlene K. Slattery [a], James M. Fenton [a]

[a] Advanced Energy Research Division, Florida Solar Energy Center, University of Central Florida, Cocoa, FL 32922, USA
[b] Center for Clean Energy Engineering, University of Connecticut, Storrs, CT 06269, USA

HIGHLIGHTS

- Ultra-low H_2 crossover showed trace oxygen dominating electrochemical response.
- The effect of scan rate on H_2 crossover was examined.
- Electrochemical methods to determine H_2 crossover should consider trace oxygen.

ARTICLE INFO

Article history:
Received 9 April 2012
Received in revised form
25 June 2012
Accepted 27 June 2012
Available online 4 July 2012

Keywords:
Hydrogen crossover
Linear sweep voltammetry
PEM fuel cells
Oxygen reduction

ABSTRACT

The determination of hydrogen permeation through a polymer electrolyte membrane is often achieved through electrochemical methods, under the assumption of no oxygen at the working electrode. However, multiple experiments utilizing low hydrogen crossover conditions have shown reduction currents resulting from trace amounts (2–3 ppm) of oxygen. For conventional membranes, hydrogen crossover is sufficient to overwhelm the trace oxygen, such that the hydrogen permeation results are unaffected. For those conditions with low hydrogen crossover, the presence of trace oxygen can become dominant. This is particularly relevant for advanced polymer electrolyte membranes with very low gas permeability. The use of electrochemical techniques to ascertain the hydrogen permeation coefficient for membranes with low gas permeability was found to be significantly influenced by the presence of trace oxygen.

1. Introduction

Hydrogen-fed polymer electrolyte membrane (PEM) fuel cells are considered to be good candidates for future power sources, for both stationary and automotive applications. They are limited in their wide-spread adoption, however, due to high costs associated with the catalyst and membrane, low performance at high temperature/low relative humidity, as well as their long-term durability [1,2]. A key component in both performance and durability is the hydrogen crossover, which is that amount of hydrogen that permeates through the membrane from the anode to the cathode. The presence of hydrogen at the cathode of an operating fuel cell can lead to significant performance losses, increased membrane degradation, as well as sudden (and catastrophic) cell failure.

Ex-situ tests have been utilized to determine the hydrogen permeation through Nafion® membranes. Determination of the hydrogen diffusing through the membrane can be through volumetric [3,4], time-lag [5,6], gas chromatography [7] and electrochemical techniques [8–12]. For in-situ measurements of hydrogen crossover in PEM fuel cells, electrochemical techniques are widely employed, making use of the electrodes within the membrane electrode assembly [13]. In these techniques, hydrogen is fed to the fuel cell anode (which serves as a pseudo-reference/counter electrode) while pure N_2 or Ar is fed to the fuel cell cathode (i.e. working electrode). A voltage is applied between the counter and working electrodes, and the resultant currents are measured. In the presence of crossover hydrogen, an oxidizing current will be present due to the oxidation of H_2 to two electrons and two protons. At a sufficiently high voltage (>0.3 V), the rate of H_2 oxidation will be limited by the diffusion of H_2 through the membrane, resulting in a limiting current. Hydrogen crossover is often reported as this limiting current, which can be on the order of 1–2 mA cm^{-2} for 25 μm thick DuPont Nafion® membranes at 25 °C [14]. Various factors, including membrane material, membrane thickness, water content, and hydrogen partial pressures, will contribute to the hydrogen crossover limiting current.

As membrane development continues, there is a drive to manufacture thinner membranes with decreased gas crossover. As

* Corresponding author. Tel.: +1 321 638 1478; fax: +1 321 638 1010.
E-mail address: pbrooker@fsec.ucf.edu (R.P. Brooker).

0378-7753/$ – see front matter © 2012 Elsevier B.V. All rights reserved.
http://dx.doi.org/10.1016/j.jpowsour.2012.06.089

the membrane becomes thinner, the ohmic losses associated with proton conduction through the membrane will decrease and water management will be simplified, but the hydrogen crossover will increase due to a reduced diffusion length. With increased hydrogen crossover, membrane degradation will increase due to increased platinum band formation and hydroxyl radical generation [13,15]. Therefore, membranes are being developed with lower gas crossover rates in order to reduce these effects.

There are some practical considerations that have been observed by the authors for these low-crossover membranes. In particular, the authors have observed, on multiple occasions, reduction currents during linear sweep voltammetry (LSV). For example, the use of 50 μm thick sulfonated polyetheretherketone (SPEEK) membranes resulted in a reduction current, even though the experimental conditions were similar to those tests with NRE 211 that gave oxidation currents [16]. As it relates to determining hydrogen crossover, utilizing electrochemical methods would result in "negative crossover" (a physical impossibility) when these reduction currents are present. These results caused the authors to consider what factors give rise to reduction currents in LSVs, since these currents could impact the reliability of electrochemical techniques for H_2 crossover measurements for low-crossover membranes. In this study, low crossover was simulated through the use of dilute hydrogen.

2. Experimental method

A 5 cm^2 catalyst coated membrane (CCM) was prepared from an NRE 211 membrane (DuPont) by spraying catalyst ink using an airbrush (Badger). The final electrode composition (both anode and cathode) was 28% ionomer (available from 3M company) with PtCo/C catalyst from Tanaka (46% Pt, 4.6% Co, TKK, Japan). The CCM was assembled into single-pass serpentine fuel cell hardware (Fuel Cell Technology), with SGL 10BC gas diffusion layers (Sigracet) and 225–250 μm pinch. The cell was operated at 25 °C/100% RH for several LSVs until stable results were obtained (i.e. multiple hours of tests).

All experiments used Ultra High Purity (UHP) N_2 at the working electrode, while the counter electrode had either 4% H_2/96% Ar ("dilute H_2"), 100% UHP H_2 ("pure H_2"), or UHP N_2 flowing. Air used in cathode-sparger purging was zero grade. Gas flow rates were set at 0.17 L min^{-1}, with cell and saturator temperatures all set to 25 °C.

For each experiment, the fuel cell anode served as the pseudo-reference/counter electrode, while the fuel cell cathode was the working electrode. Using a PAR 263 potentiostat (Princeton Applied Research, Oak Ridge, TN, high current option installed), linear sweep voltammograms (LSVs) were conducted, scanning the voltage between 0.01 and 0.5 V, at sweep rates of 1, 2, or 4 mV s^{-1}. For those LSVs where the OCV with dilute H_2/N_2 was high (i.e. >0.1 V), in order for the experiment to proceed, the cell had to be briefly shorted out by connecting the leads from each electrode. After disconnecting the leads, the voltage would slowly climb, reaching the previous voltage within 5 min. If the LSV experiment was started when the voltage was high, the potentiostat current limits would be reached, and the experiment would end. However, if the LSV was started while the voltage was still low, no problems were encountered. Therefore, whenever the voltage was greater than 0.1 V, the cell would be briefly shorted out prior to starting the LSV.

Cyclic voltammograms (CVs) were conducted by scanning the voltage between 0.01 and 0.8 V at a sweep rate of 30 mVs^{-1}, with the initial voltage for all CVs equal to the OCV, e.g. 0.092 V for pure H_2/N_2 and >0.7 V for dilute H_2/N_2. The hydrogen adsorption region was determined as that area under the reduction curve (after correcting for double-layer charging) between approximately 0.08 and 0.4 V. Electrochemically active surface area (ECA) was determined from this adsorption area and assumed 210 μC cm^{-2} Pt charge for a monolayer adsorption of hydrogen. Oxide surface area was determined from the area under the curve during the first reduction sweep, and was taken between approximately 0.5 and 0.7 V, assuming 210 μC cm^{-2} as the charge of adsorption. The fraction of oxide on the platinum surface was determined from the ratio of the oxide area to the hydrogen area. Mid-line currents from CVs were determined by taking the average current between the cathodic and anodic sweeps at 0.4 V.

Diffusion coefficients were determined from the limiting current obtained from the LSVs and CVs, through the use of Fick's Law, assuming a linear concentration profile, and applying Henry's law to relate concentration with pressure, resulting in Eq. (1):

$$j_{x-\text{over}} = \Psi_{H_2} * \Delta P / \Delta x \quad (1)$$

where: $j_{x\text{-over}}$ = hydrogen crossover, in mol s^{-1} cm^{-2}. Ψ_{H2} = hydrogen permeation coefficient, in mol s^{-1} cm^{-1} atm^{-1}. ΔP = Hydrogen partial pressure difference between anode and cathode electrodes, in atm. Δx = membrane thickness, in cm.

It was assumed that the partial pressure of hydrogen at the cathode side is zero. This is justified given that any crossover hydrogen from the anode will immediately be oxidized at the working electrode's elevated potential.

3. Results

The test stand that was used for these experiments had not been used with air for more than two weeks, and had remained idle for the week immediately preceding testing. During the first 4 min after the stand was turned on, the only gases flowing were N_2/N_2 (anode/cathode), with an OCV of about 0.03 V. At the 4-min mark, the anode gas was switched to dilute H_2, and the OCV climbed to 1 V 1 min later. The stand was allowed to purge with dilute H_2/N_2 for an additional 2 min, and then an LSV was obtained (LSV_{7min}, see Fig. 1). As mentioned above, the cell was shorted to reduce the cell voltage to near zero prior to the LSV. The current measured during

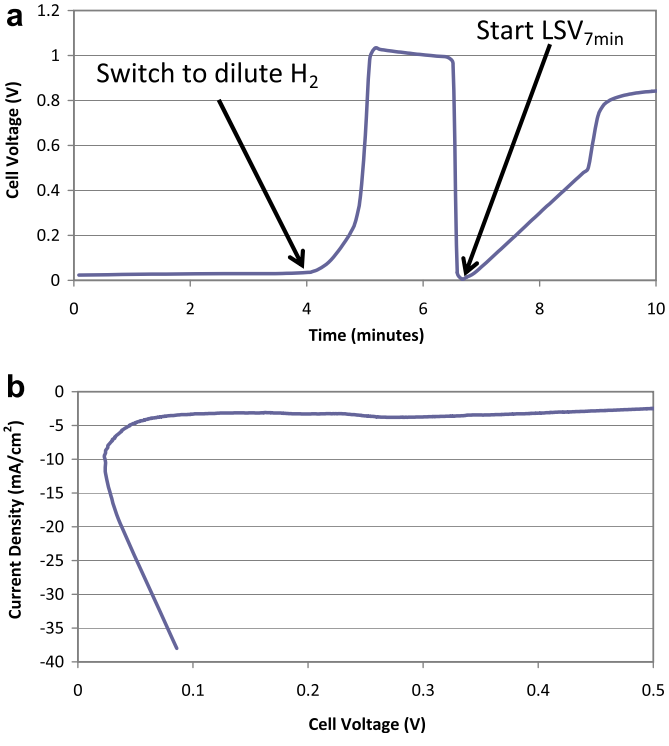

Fig. 1. (a) Cell voltage vs. time during startup. (b) LSV_{7min} results. Conditions: dilute H_2, 25 °C/100% RH, 4 mV s^{-1}.

this LSV was negative, indicative of a reduction process at the working electrode.

From the increase in voltage after switching to dilute H_2/N_2, it seems as though a small amount of oxygen is present in the system. This would also explain the negative current during LSV_{7min}. It also appears as though the concentration of O_2 is decreasing with time, as evidenced by the slow decrease in OCV between 5 and 6 min in Fig. 1(a), and in the gradual increase in current during LSV_{7min}. To confirm the gradual decrease in O_2 concentration, LSVs were obtained at 16, 21 and 31 min after startup (see Fig. 2).

Between 7 and 16 min after startup, there is still sufficient oxygen in the system to provide negative currents due to O_2 reduction at the working electrode. After 21 min, a positive current appears, indicative of hydrogen oxidation at the working electrode and consequently less oxygen reduction. At 31 min, the current is more positive, suggesting greater hydrogen oxidation.

To examine further the effect of purging time on LSVs, the cathode gas line was disconnected from the cell, and the cell was capped, with no flow through the anode either. Air was purged through the cathode sparger of the test stand at 0.4 L min^{-1} for 7 min, followed by a purge with N_2 for an additional 7 min. Then, the gas flow was stopped, the line was reconnected to the cell, gas flow was started at 0.17 L min^{-1} through the cell and LSVs were obtained at 8, 14, 26, and 50 min after the air purge ended (see Fig. 3).

As the air is purged from the sparger, the currents associated with oxygen reduction decrease, with very little change between 26 and 50 min. To confirm that the oxygen concentration has reached steady state, the anode and cathode spargers were purged with N_2/N_2 for 1 h, then an LSV with dilute H_2/N_2 was obtained (i.e. at the 120 min mark). As can been seen in Fig. 4, there is little

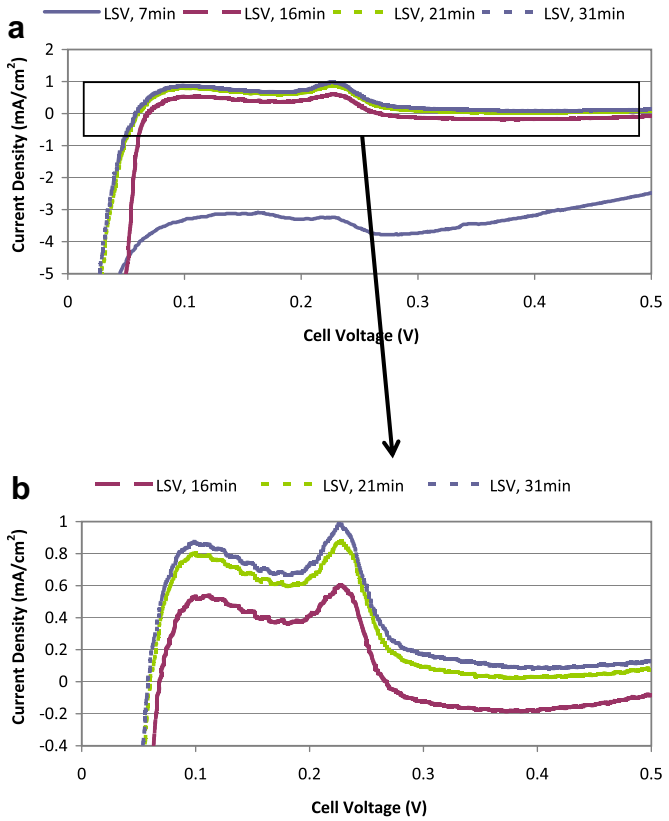

Fig. 2. (a) LSV results from 7, 16, 21, and 31 min. (b) Expanded region from (a). Conditions: dilute H_2, 25 °C/100% RH, 4 mV s^{-1}.

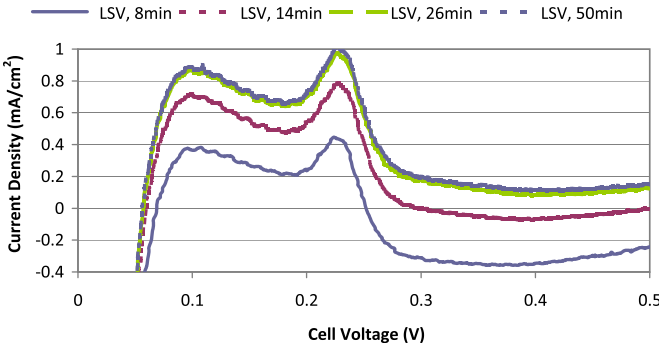

Fig. 3. LSVs obtained after air saturator purge. Conditions: dilute H_2, 25 °C/100% RH, 4 mV s^{-1}.

change, indicating the oxygen concentrations are stable after about 30 min.

The presence of an oxidation current in Fig. 4 does not indicate the absence of oxygen in the N_2 stream. It will be shown later that the scan rate of the LSV influences the current. Therefore, it is possible that oxygen is still present after this long purge.

To test this hypothesis, the same experiments conducted in Fig. 3 were repeated, only using cyclic voltammetry. In this approach, the presence of oxygen may be visualized in the production of oxides. The results from the CV experiments are shown in Fig. 5. The ECA, amount of oxide and fractional oxide coverage from each experiment are listed in Table 1. Additionally, the mid-line current from each CV was determined, as it is theorized that this line is equivalent to the hydrogen crossover current. This can be justified due to the capacitive nature of the electrodes causing double-layer charging and discharging during the oxidation and reduction sweeps. As sweep rates increase, the capacitive charging will also increase. The average current between the oxidation and reduction currents at 0.4 V represents a sweep rate of 0 mV s^{-1}, which will only be influenced by the hydrogen crossover. Cheng et al. used this method to determine the hydrogen crossover of cells subjected to accelerated stress tests [17].

From these CV experiments, it appears that after the cathode sparger air purge, a significant amount of oxygen remains in the system to create an oxide layer on the surface of platinum. As was observed with the LSV experiments the amount of oxygen present decreases with time. This is observed in both the reduction in oxide coverage and the shift to more positive mid-line currents. However, unlike the LSV results, the mid-line currents remain negative even after 41 min, where the oxygen concentration was found to be at steady state. This suggests that there is still oxygen present after purging for long times. It has been reported that the formation of oxides on platinum is dependent on water and voltage [18]. In the

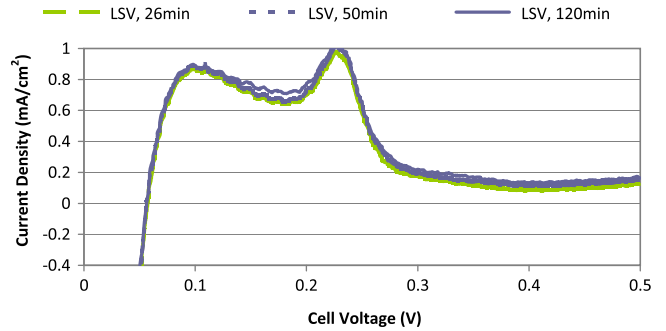

Fig. 4. LSVs obtained 26, 50 and 120 min after air purge. Conditions: dilute H_2, 25 °C/100% RH, 4 mV s^{-1}.

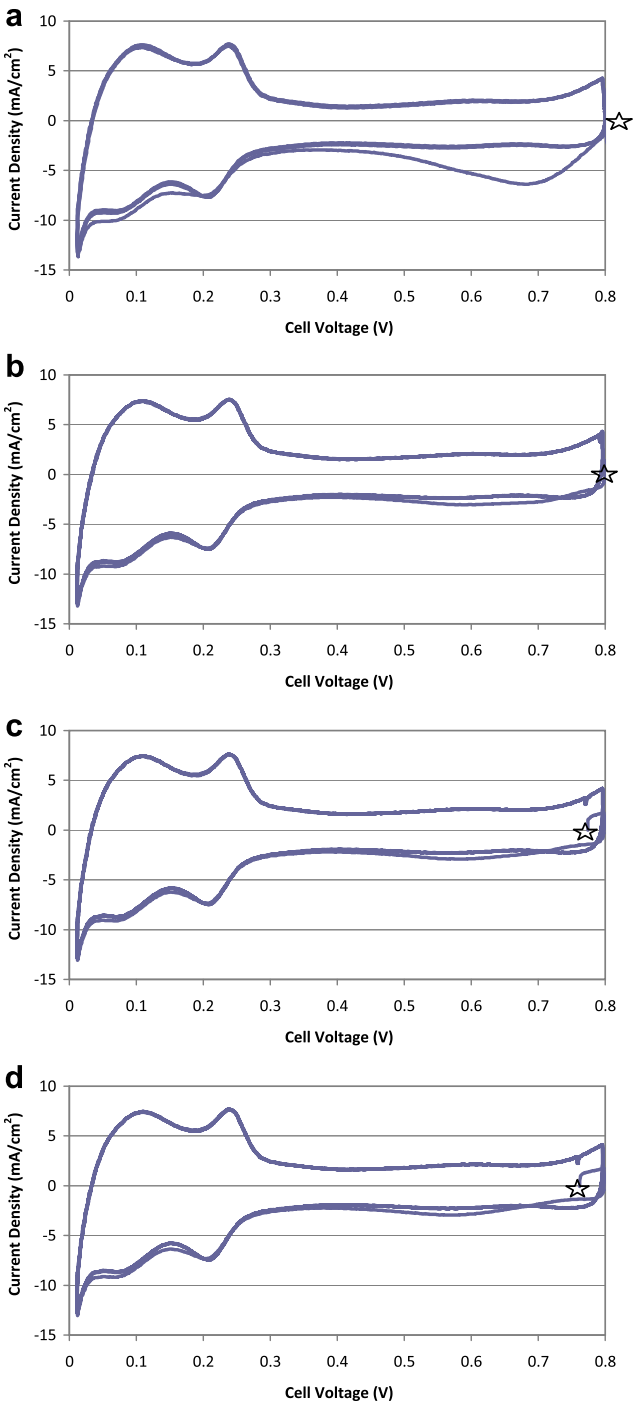

Fig. 5. CVs obtained at (a) 8 min, (b) 16 min, (c) 26 min and (d) 41 min after air purge. Starting OCVs are marked with a star, and are (a) 0.839 V, (b) 0.795 V, (c) 0.773 V and (d) 0.761 V. Conditions: dilute H_2, 25 °C/100% RH, 30 mV s^{-1}.

present study, it appears as though oxide formation may be occurring because trace oxygen maintains an elevated potential, where water can oxidize on the surface of platinum. The Nernst equation predicts that as little as 1 ppm O_2 can result in an OCV of 1.1 V. The OCVs in this study occasionally reached 1 V, but often were above 0.7 V with dilute H_2. In Fig. 5, the starting OCVs are marked with stars, and it can be seen that the OCV was slowly decreasing, indicative of decreasing oxygen concentrations at the cathode. The equilibrium amount of O_2 dissolved in the saturator water at 25 °C from air is approximately 2.8×10^{-4} mol L^{-1}. Purging

Table 1
Results from CV experiments after air purge.

Time after air purge	ECA (m^2 g^{-1} Pt)	Amount of oxide (mol OH)	% Oxide coverage	Mid-line current (mA cm^{-2})
8 min	55	$1.08e^{-6}$	55%	−0.57
16 min	51	$2.31e^{-7}$	12%	−0.28
26 min	51	$2.01e^{-7}$	11%	−0.19
41 min	53	$1.76e^{-7}$	9%	−0.14

with N_2 after air will reduce the amount of dissolved oxygen in the sparger, and given that O_2 is twice as soluble in water as N_2, it is believed that a considerable amount of O_2 remains after the N_2 purge. At equilibrium as little as 1.3×10^{-9} mol L^{-1} in the cathode sparger would give an O_2 concentration of 1 ppm in the cathode gas stream. It is believed that even after purging for 7 min with N_2, there is likely sufficient dissolved O_2 in the water to provide ppm-levels of O_2 in the cathode gas stream.

The question arises as to why the LSV shows a positive current, while the CVs indicate a negative current. To resolve this conflict, LSVs were obtained with different scan rates; 1, 2, and 4 mV s^{-1}. The 4 mV s^{-1} test was repeated before and after these tests and showed no change, indicating steady state had been achieved. An additional test was conducted where the voltage was held steady at 0.4 V for 30 min (i.e. equivalent to a 0 mV s^{-1} scan rate). The results from the LSV tests and constant voltage test are shown in Fig. 6. The current at 0.4 V for the LSVs, constant voltage and 41 min CV mid-line are compared in Table 2.

As scan rate decreases, the value of the current also decreases, eventually becoming negative at 1 mV s^{-1}, with the total difference in current density between the 4 mV s^{-1} and CV mid-line being 0.26 mA cm^{-2}. The constant voltage current was slightly more negative than the 1 mV s^{-1}, and most closely agrees with the CV mid-line current, which may suggest that this is the true crossover value. The dependence of current on scan rate (see Fig. 7) suggests

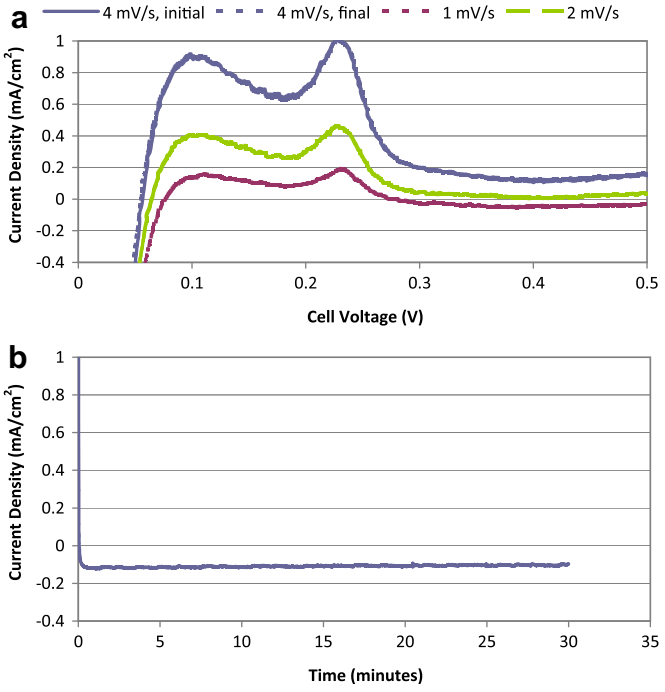

Fig. 6. (a) LSVs at 1, 2, and 4 mV s^{-1}. (b) Constant voltage (0.4 V) vs. time. Conditions: dilute H_2, 25 °C/100% RH, 4 mV s^{-1}.

Table 2
Comparison of currents for different experiments with dilute H_2.

	Const. voltage	1 mV s^{-1}	2 mV s^{-1}	4 mV s^{-1}	41 min. CV mid-line
Current at 0.4 V (mA cm^{-2})	−0.102	−0.046	0.008	0.12	−0.14

that capacitive effects are influencing the measured current. In this case, the capacitive effects were sufficient to make the difference between analyzing an oxidizing current (i.e. hydrogen crossover) and analyzing a reduction current (i.e. excess oxygen). The presence of a reduction current indicates a low-level amount of oxygen is present in the N_2 stream. The concentration of O_2 in the stream can be calculated from the negative limiting current, and is determined to be 2.9 ppm. This is on the order of the 1 ppm specification provided by the UHP N_2 supplier. The additional O_2 may originate from the dissolved oxygen in the cathode sparger water.

As a further step, the amount of H_2 crossover can be predicted using the H_2 permeation coefficient derived from a paper by Weber and Newman [19]. In this paper, a mathematical model is provided to predict the H_2 permeation coefficient based on the membrane water content. The equations require an estimate of membrane water content, which for the conditions used in the current study was assumed to be saturated from vapor at 25 °C, i.e. a λ of 14. This assumption leads to a permeation coefficient of 8.64×10^{-12} mol $cm^{-1}atm^{-1}s^{-1}$, which is in good agreement with other literature values. The permeation coefficients for hydrogen obtained from crossover values from the CV mid-line and LSVs using dilute H_2 are shown in Table 3. Clearly, a negative permeation coefficient is physically impossible, which indicates other processes (such as oxygen reduction) are dominating.

Returning to Weber's model, given that the model gives an accurate value of hydrogen crossover, and given that the current during the voltage hold was negative (i.e. −0.102 mA cm^{-2}), the amount of oxygen present at the working electrode can be estimated. The amount of oxygen present at the working electrode can be determined by hypothesizing that the negative current is an oxygen reduction limiting current and adding to that the amount of predicted H_2 crossover (i.e. from the model) that would have been consumed by oxygen. This gives a total flow rate of oxygen in the cathode stream of 4.95×10^{-10} mol s^{-1}, or 3.92 ppm. This is a very small value, but it is sufficient to significantly influence the results of very low hydrogen crossover membranes.

To investigate the impact of this trace oxygen on a conventional membrane, LSVs were obtained with pure instead of dilute H_2. LSVs (obtained at 1, 2 and 4 mV s^{-1}) and a CV were obtained with pure H_2, and the current at 0.44 V was compared (see Fig. 8 and Table 4). The selection of 0.44 V was made based on the shift in Nernst potential between pure and dilute H_2 (i.e. 41 mV), ensuring that a similar region within the LSV was examined between the two

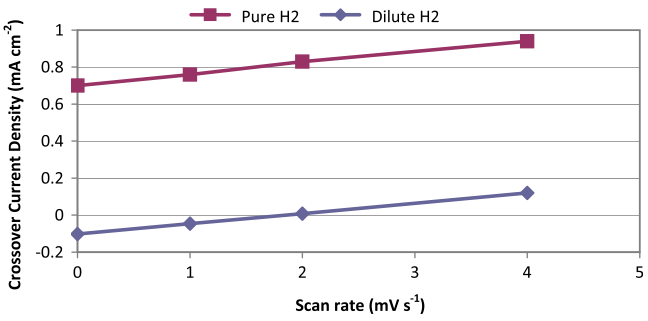

Fig. 7. Plot of crossover current as a function of scan rates for dilute and pure H_2.

Table 3
Permeation coefficients for hydrogen from CVs and LSVs with dilute and pure H_2.

H_2 concentration	CV mid-line	1 mV s^{-1}	2 mV s^{-1}	4 mV s^{-1}
Dilute	−3.47E−11	−1.56E−11	2.72E−12	4.08E−11
Pure	9.51E−12	1.03E−11	1.13E−11	1.28E−11
Theoretical	*8.64E−12*			

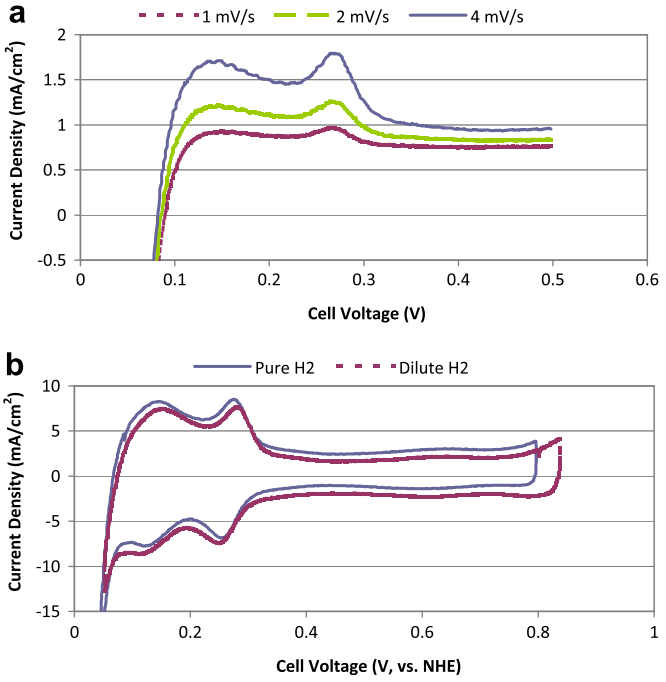

Fig. 8. (a) LSVs at 1, 2, and 4 mV s^{-1} with pure H_2. (b) CV with pure and dilute H_2.

conditions. The ECA determined from the CVs with pure H_2 was 51.6 m^2 g^{-1} Pt, which is identical to that determined with dilute H_2 (51.4 m^2 g^{-1} Pt).

As was seen for the dilute H_2 case, the lower scan rates give a lower current, with the total difference between the CV mid-line and 4 mV s^{-1} rate being 0.24 mA cm^{-2}. The dependence of current on scan rate indicates again a capacitive effect is significantly contributing to this response. In the case of pure hydrogen at the counter electrode, the capacitive effect could account for more than 25% of the measured hydrogen crossover using a scan rate of 4 mV s^{-1}. The permeation coefficients were determined from the crossover obtained from all LSVs, as well as from the CV mid-line current (see Table 3). As can be seen, the CV mid-line provided the closest agreement to theoretical values.

The fact that for pure H_2 the CV did not show any oxide peaks, and that the OCV was so low (0.092 V) suggests that using pure H_2 provides sufficient crossover to react any trace oxygen from the surface of the working electrode, thereby lowering the OCV and preventing oxide formation. If the estimate for oxygen concentration from the dilute case is included in the analysis with the pure H_2 case, the permeation coefficient will increase from 9.51 to 9.61 mol s^{-1} cm^{-1} atm^{-1}, an increase of about 1%.

Table 4
Comparison of currents for different experiments with pure H_2.

	1 mV s^{-1}	2 mV s^{-1}	4 mV s^{-1}	CV mid-line
Current at 0.44 V (mA cm^{-2})	0.76	0.83	0.94	0.70

4. Conclusions

The use of electrochemical methods to determine permeation coefficients will be influenced by both the scan rate for LSVs as well as the trace amounts of oxygen in the gas stream at the working electrode. This is particularly true for low-crossover membranes, where trace O_2 can consume all the crossover hydrogen, with residual O_2 to create reduction currents. Negative currents during LSVs were observed when trace amounts of oxygen are present (i.e. on the order of 2–4 ppm), but only when very little H_2 crosses over to the working electrode, as was observed for the case where dilute H_2 is used. It is expected that similar effects will be observed when low gas-crossover membranes are employed, e.g. SPEEK. Trace oxygen may originate from the gas source as well as out-gassing from the cathode sparger. Therefore, when investigating hydrogen crossover for advanced membranes with low H_2 permeability, gases should be used with as low an oxygen concentration as possible. Reducing exposure of the cathode sparger water to oxygen will also reduce the amount of oxygen in the cathode gas stream. Additionally, it was found that the scan rate during the LSV can influence the measured crossover value by as much as 25% with pure H_2, and even changes the analysis with dilute H_2. Using the mid-line current from a CV or employing a voltage hold will be more accurate.

Acknowledgements

The authors wish to acknowledge the US Department of Energy for funding this research.

References

[1] F.A. de Bruijn, V.A.T. Dam, G.J.M. Janssen, Fuel Cells (Weinheim, Ger.) 8 (2008) 3–22.
[2] J. Wu, X.Z. Yuan, J.J. Martin, H. Wang, J. Zhang, J. Shen, S. Wu, W. Merida, J. Power Sources 184 (2008) 104–119.
[3] T. Sakai, H. Takenaka, N. Wakabayashi, Y. Kawami, E. Torikai, J. Electrochem. Soc. 132 (1985) 1328–1332.
[4] A.B. LaConti, A.R. Fragala, J.R. Boyack, Proc. Electrochem. Soc. 77 (6) (1977) 354–374.
[5] T. Sakai, H. Takenaka, E. Torikai, J. Electrochem. Soc. 133 (1986) 88–92.
[6] T. Sakai, H. Takenaka, E. Torikai, J. Membr. Sci. 31 (1987) 227–234.
[7] K. Broka, P. Ekdunge, J. Appl. Electrochem. 27 (1997) 117–123.
[8] R.S. Yeo, J. McBreen, J. Electrochem. Soc. 126 (1979) 1682–1687.
[9] Z. Ogumi, Z. Takehara, S. Yoshizawa, J. Electrochem. Soc. 131 (1984) 769–773.
[10] Z. Ogumi, T. Kuroe, Z. Takehara, J. Electrochem. Soc. 132 (1985) 2601–2605.
[11] Y.M. Tsou, M.C. Kimble, R.E. White, J. Electrochem. Soc. 139 (1992) 1913–1917.
[12] A.T. Haug, R.E. White, J. Electrochem. Soc. 147 (2000) 980–983.
[13] M. Inaba, T. Kinumoto, M. Kiriake, R. Umebayashi, A. Tasaka, Z. Ogumi, Electrochim. Acta 51 (2006) 5746–5753.
[14] S.S. Kocha, J. Deliang Yang, J.S. Yi, AICHE J. 52 (2006) 1916–1925.
[15] V.A. Sethuraman, J.W. Weidner, A.T. Haug, L.V. Protsailo, J. Electrochem. Soc. 155 (2008) B119–B124.
[16] S.L.N.H. Rhoden, C.A. Linkous, N. Mohajeri, D.J. Díaz, P. Brooker, D.K. Slattery, J.M. Fenton, J. Membr. Sci. 376 (2011) 290–301.
[17] T.T.H. Cheng, E. Rogers, A.P. Young, S. Ye, V. Colbow, S. Wessel, J. Power Sources 196 (2011) 7985–7988.
[18] H. Xu, R. Kunz, J.M. Fenton, Electrochem. Solid-State Lett. 10 (2006) B1–B5.
[19] A.Z. Weber, J. Newman, J. Electrochem. Soc. 151 (2004) A311–A325.

Glossary

PEM: polymer electrolyte membrane
LSV: linear sweep voltammetry
CV: cyclic voltammetry
OCV: open circuit voltage
ECA: electrochemically active area
CCM: catalyst coated membrane